

**CO<sub>2</sub> Sequestration and Recycle by Photosynthesis**

**Technical Progress Report**

**September 24, 2004 – Septemeber 23, 2005**

Steven S. C. Chuang

February 12, 2006

Department of Chemical Engineering, The University of Akron

200 East Buchtel Commons

Akron, OH, 44325-3906

Phone number: 330-972-6993; Fax number: 330-972-5856

E-mail: [schuang@uakron.edu](mailto:schuang@uakron.edu)

DE-PS26-01NT41294

**Disclaimer**

This report was prepared as an account of work sponsored by an agency of the United States Government. Neither the United States Government nor any agency thereof, nor any of their employees, makes any warranty express or implied, or assumes any legal liability or responsibility for the accuracy, completeness, or usefulness of any information, apparatus, product, or process disclosed, or represents that its use would not infringe privately owned rights. Reference herein to any specific commercial product, process, or service by trade name, trademark, manufacturer, or otherwise does not necessarily constitute or imply its endorsement, recommendation, or favoring by the United States Government or any agency thereof. The views and opinions of authors expressed herein do not necessarily state or reflect those of the United States Government or any agency thereof.

## **ABSTRACT**

Hydrocarbon oxygenate synthesis from photocatalytic reactions of CO<sub>2</sub> and H<sub>2</sub>O over various catalysts is a very attractive process. However, the formation rate of the hydrocarbons and oxygenates is significantly lower than conventional catalysis. One possible reason for the low rate of product formation is the presence of oxidation sites which reoxidize the products back to CO<sub>2</sub> and H<sub>2</sub>O. For further improvement of catalytic activity for the reduction process, it is essential to understand the oxidation reaction process. We have studied photocatalytic oxidation of methylene blue and found the oxidation rate is significantly higher than the reduction rate.

## **TABLE OF CONTENTS**

ABSTRACT.....	2
LIST(S) OF GRAPHICAL MATERIALS.....	4
INTRODUCTION.....	5
EXECUTIVE SUMMARY.....	5
EXPERIMENTAL.....	6
RESULTS AND DISCUSSION.....	7
CONCLUSIONS.....	9
REFERENCES.....	10

## LIST(S) OF GRAPHICAL MATERIALS

Figure 1	Schematic diagrams of MB photocatalytic oxidation on Diffuse Reflectance Infrared Fourier Transform Spectroscopy reactor.....	11
Figure 2	XRD patterns of pure TiO <sub>2</sub> , 0.5 wt% Pt/TiO <sub>2</sub> , 1 wt% Pt/TiO <sub>2</sub> and 3 wt% Pt/TiO <sub>2</sub> . A and R designate anatase and rutile respectively.....	12
Figure 3	UV-vis diffuse reflectance spectra of pure TiO <sub>2</sub> , 0.5 wt% Pt/TiO <sub>2</sub> , 1 wt% Pt/TiO <sub>2</sub> and 3 wt% Pt/TiO <sub>2</sub> .....	13
Figure 4	Concentrations of MB as a function of time in photocatalytic oxidations of MB in aqueous solution with non-catalyst, pure TiO <sub>2</sub> , and 0.5 wt% Pt/TiO <sub>2</sub> .....	14
Figure 5	Photocatalytic oxidation of MB in liquid-thin film system with non-catalyst, P25, and 0.5 wt% Pt/P25.....	15
Figure 6	IR backgrounds of CaF <sub>2</sub> and MB/CaF <sub>2</sub> , TiO <sub>2</sub> and MB/TiO <sub>2</sub> , 0.5 wt% Pt/TiO <sub>2</sub> and MB/0.5 wt% Pt/TiO <sub>2</sub> .....	16
Figure 7	In situ DRIFTS spectra and band assignments of MB photocatalytic oxidation over pure TiO <sub>2</sub> .....	17
Figure 8	In situ DRIFTS spectra and band assignments of MB photocatalytic oxidation over 0.5 wt% Pt/TiO <sub>2</sub> .....	18
Figure 9	Decrease rates of MB characteristic bands as a function of time in the MB photocatalytic oxidation over pure TiO <sub>2</sub> and 0.5 wt% Pt/TiO <sub>2</sub> .....	19

## **INTRODUCTION**

TiO<sub>2</sub> is the most widely studied photocatalyst because of its stability, low cost, and non-toxicity. TiO<sub>2</sub> exhibits the photocatalytic activity for both oxidation and reduction. Photocatalytic oxidation usual involves oxidation of organic species to CO and H<sub>2</sub>O in the presence of H<sub>2</sub>O or O<sub>2</sub> while photocatalytic reduction converts CO<sub>2</sub>/H<sub>2</sub>O back to hydrocarbons/oxygenates or reduces H<sub>2</sub>O to H<sub>2</sub> and O<sub>2</sub>. Examination of literature results shows that the rates of photocatalytic reduction are 3 to 4 orders of magnitude lower than those of photocatalytic oxidation. Significant enhancement in the rate of photocatalytic reduction is needed to bring this reaction process for practical applications.

One possible reason for the low rate of the photocatalytic reduction is the presence of oxidation sites on the TiO<sub>2</sub> surface which further converts hydrocarbon/oxygenate products back to CO<sub>2</sub> and H<sub>2</sub>O. A fundamental understanding of the reaction mechanism could assist in identifying key factors in improving Ti-based catalysts for controlling photocatalytic oxidation and reduction. To develop a better understanding of photocatalytic oxidation, we have studied photocatalytic oxidation of methylene blue (MB). MB is an excellent model compound for investigation of photocatalytic oxidation mechanism for (i) easy of determination of it conversion with UV-vis spectrophotometry and (ii) existence of abundant rate data for comparison.

## **EXECUTIVE SUMMARY**

This study shows that the photocatalytic oxidation activity of TiO<sub>2</sub>– based catalysts is significantly higher than their photocatalytic reduction rate. Selective inhibition of photocatalytic oxidation is needed to improve the overall rate of the photocatalytic reduction

process.

## **EXPERIMENTAL**

TiO<sub>2</sub> was supplied by Degussa (P-25, surface area ~50 m<sup>2</sup>/g; mean diameter ca. 30 nm; 80% anatase and 20% rutile); Methylene Blue (C<sub>16</sub>H<sub>18</sub>ClN<sub>3</sub>S•3H<sub>2</sub>O) from Alfa Aesar. Both compounds were used without further treatment.

### **Catalyst Preparation and Characterization**

0.5 wt % Pt/TiO<sub>2</sub> was prepared by photo-reduction of K<sub>2</sub>PtCl<sub>6</sub> onto TiO<sub>2</sub> in a solution containing ethanol which serves as a sacrificial electron donor. The specific procedure involves (i) bubbling N<sub>2</sub> through a 0.1 M ethanol solution containing K<sub>2</sub>PtCl<sub>6</sub> and TiO<sub>2</sub> particles to remove O<sub>2</sub>, (ii) illuminating the solution with a 350 W mercury UV lamp (Oriel 6286) for 24 hours while suspending TiO<sub>2</sub> particle in the solution by magnetic bar stirring, (iii) removal of Pt/TiO<sub>2</sub> from the solution by centrifuging, (iv) washing the particle with deionized water to remove Cl and K ion, (v) and drying under vacuum oven at 100 °C. TiO<sub>2</sub> and 0.5 wt% Pt/TiO<sub>2</sub> were characterized by X-ray diffraction (Phillips APD3700 X-ray diffractometer equipped with a Cu K<sub>α</sub> radiation source giving a wavelength of 1.5406 Å) and UV-Vis spectroscopy UV-Visible spectrophotometer (HITACHI U-3010) equipped with a Praying Mantis diffuse reflectance accessory.

### **Photocatalytic Degradation of Methylene Blue in an Aqueous Solution**

Photocatalytic degradation of Methylene Blue was studied with on two different modes. The first involves a square quartz reactor containing a 50 ml aqueous solution suspending with 5

mg of the catalysts under magnetic stirring; the second involves immobilizing the TiO<sub>2</sub> by coating it on one side of the reactor wall by a slurry deposition technique. The concentration of MB was determined by UV-Vis spectroscopy.

### In situ Infrared Study

Fig. 1 illustrates the experimental approaches used for the in situ infrared study. 50 mg of the reactant/catalyst mixture was placed in a DRIFT (diffuse reflectance) cell and then exposed to a light from Xe lamp with an intensity of 16.7 mW/cm<sup>2</sup>. DRIFT spectrum was taken by closing the movable light collector and interrupting the photocatalytic reaction,

## RESULTS AND DISCUSSION

### Characterization

Figure 2 shows the XRD patterns of TiO<sub>2</sub>, 0.5 wt% Pt/TiO<sub>2</sub>, 1 wt% Pt/TiO<sub>2</sub>, and 3 wt% Pt/TiO<sub>2</sub>. XRD results shows that TiO<sub>2</sub> contains both anatase and rutile, confirming the P-25 structure; increasing the Pt content leads to an increase in the intensity of the Pt (111) peak at 39.8°. The absence of Pt peak in 0.5 wt% TiO<sub>2</sub> suggests the Pt particle size on 0.5 wt% Pt/TiO<sub>2</sub> is less than 3 nm.

Figure 3 shows the results of the diffuse reflectance UV-Vis spectra of the TiO<sub>2</sub>, 0.5 wt% Pt/TiO<sub>2</sub>, 1 wt% Pt/TiO<sub>2</sub>, and 3 wt% Pt/TiO<sub>2</sub>. TiO<sub>2</sub> gave the absorption edge at 450 nm. The addition of Pt shifted the absorption edge to the lower wavelength and decreased the absorption. The latter could be resulted from increases in reflection from Pt metal particles.

### Aqueous Phase Kinetic Study

Figure 4 shows the kinetics of MB photocatalytic degradation in an aqueous solution with suspending TiO<sub>2</sub> and 0.5 wt% Pt/TiO<sub>2</sub> particles. The rate of disappearance of MB fit well into the first order kinetics as shown in Fig. 5. This could be due to the presence of the significant excess H<sub>2</sub>O which reduces the kinetic rate law into the pseudo first order form. The rate constant obtained from fitting, listed in Table 1, is in the same order of magnitude with those reported in literature. In general, the rate constant depends on the catalyst composition and concentration as well as the wavelength and intensity of the illuminating light. Results in Fig 4 and Table 1 show increasing the catalyst concentration increased the rate constant. The addition of Pt had little effect on the MB degradation.

Figure 5 shows the kinetics of MB degradation in an aqueous solution on TiO<sub>2</sub> and 0.5 wt% Pt/TiO<sub>2</sub> coating on the reactor wall. The objective of this study is to determine the photocatalytic oxidation kinetics in the absence of screening effect of the catalyst particles. The initial MB concentration was 30 ppm in the aqueous solution. 1.2 mg catalyst was coated on a surface of 4.5 cm<sup>2</sup>

#### In situ Infrared Study

Figure 6 shows the key characteristic IR bands of MB on CaF<sub>2</sub>, TiO<sub>2</sub>, and 0.5wt% Pt/TiO<sub>2</sub>. Methylene blue exhibits the aromatic ring C=C/C=N at 1599 cm<sup>-1</sup>, C=C at 1488 cm<sup>-1</sup>, C-H at 1388 cm<sup>-1</sup>, the aromatic amine C<sub>Ar</sub>-N at 1332 cm<sup>-1</sup>, and the C-H wagging at 1250 cm<sup>-1</sup>. The bands in 1400 – 1600 cm<sup>-1</sup> became obscure for methylene blue on both TiO<sub>2</sub> and 0.5 wt% Pt/TiO<sub>2</sub> due to the strong IR absorption background of the TiO<sub>2</sub> catalysts. The IR bands observed in Figure 6 are summarized in Table 2. Both TiO<sub>2</sub> and Pt/TiO<sub>2</sub> exhibited a number of OH groups. These bands were attenuated after impregnating MB onto the catalysts.

Figure 7 shows the DRIFT spectra of MB on TiO<sub>2</sub> during photocatalytic degradation. Exposure of MB on TiO<sub>2</sub> to the UV illumination led to: (i) decrease in IR intensity of all the above bands as well as C-H at 2931 cm<sup>-1</sup> and C=C in the aromatic ring at 1488 cm<sup>-1</sup>; (ii) increase in IR intensity of the bands of C=O at 1718 cm<sup>-1</sup> and N-H at 1576 cm<sup>-1</sup>. The IR results suggested that MB photocatalytic oxidation proceeded the intermediates containing carbonyl functional group (C=O) and produced ammonium ion (NH<sup>4+</sup>). Figure 8 shows photocatalytic degradation of MB on 0.5 wt% Pt/TiO<sub>2</sub>. To compare the difference in the rate of change in IR intensity for both TiO<sub>2</sub> and 0.5 wt% Pt/TiO<sub>2</sub>, the IR intensity of the MB bands was plotted in Figure 9. The presence of Pt accelerated the rate of decreases in the C<sub>Ar</sub>-N band at 1332 cm<sup>-1</sup> and increased the rate of formation of the N-H band at 1576 cm<sup>-1</sup>.

## CONCLUSIONS

Pt has been shown to be effective in promoting photocatalytic reactions. This study shows that Pt promotes photocatalytic oxidation of MB on TiO<sub>2</sub>. However, the presence of the aqueous phase diminishes the Pt effect. The high rate of photocatalytic oxidation suggests that the electron and hole separation do take place at an appreciable rate. The low rate of photocatalytic reduction reaction process can not be attributed to the low efficiency of electron and hole separation. The low rate of photocatalytic reduction process could be due to lack of the site to transfer of electron and hole to the desirable adsorbed species.

## REFERENCES:

1. Zhang, T.; Oyama, T.; Aoshima, A.; Hidaka, H.; Zhao, J.; Serpone, N., *Journal of Photochemistry and Photobiology A: Chemistry*, 140, 163 (2001).
2. Lachheb, H.; Puzenat, E.; Houas, A.; Ksibi, M.; Elaloui, E.; Guillard, C.; Herrmann, J., *Applied Catalysis B: Environmental*, 39, 75 (2002).
3. Zhang, T.; Oyama, T.; Horikoshi, S.; Hidaka, H.; Zhao, J.; Serpone, N., *Solar Energy Materials & Solar Cells*, 73, 287 (2002).
4. Lakshmi, S.; Renganathan, R.; Fujita, S., *Journal of Photochemistry and Photobiology A: Chemistry*, 88, 163 (1995).
5. Supsakulchai, A.; Ma, G.; Nagai, M.; Omi, S., *J. Microencapsulation*, 20, 19 (2003).
6. Inagaki, M.; Imai, T.; Yoshikawa, T.; Tryba, B., *Applied Catalysis B: Environmental*, 51, 247 (2004).
7. Li, X.; Li, F.; Yang, C.; Ge, W., *Journal of Photochemistry and Photobiology A: Chemistry*, 141, 209 (2001).
8. Li, F.; Li, X., *Chemosphere*, 48, 1103 (2002).
9. Li, F.; Li, X., *Applied Catalysis A: General*, 228, 15 (2002).
10. Li, X.; Li, F., *Environ. Sci. Technol.*, 35, 2381 (2001).

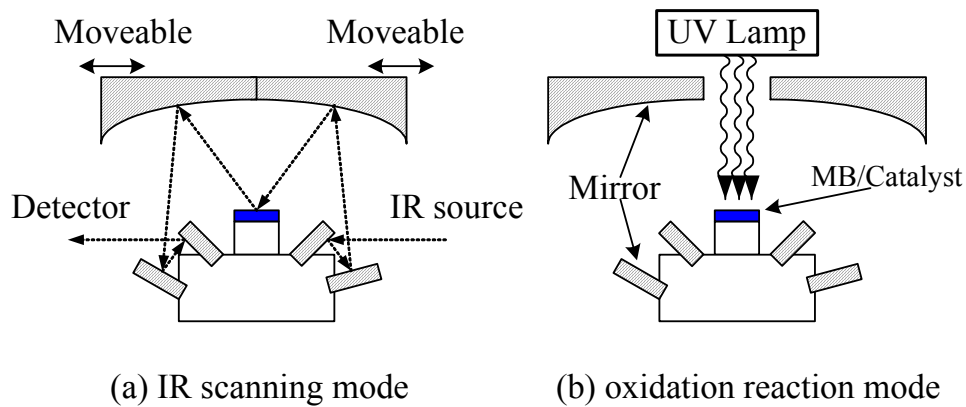


Fig. 1. Schematic diagrams of MB photocatalytic oxidation on Diffuse Reflectance Infrared Fourier Transform Spectroscopy reactor.

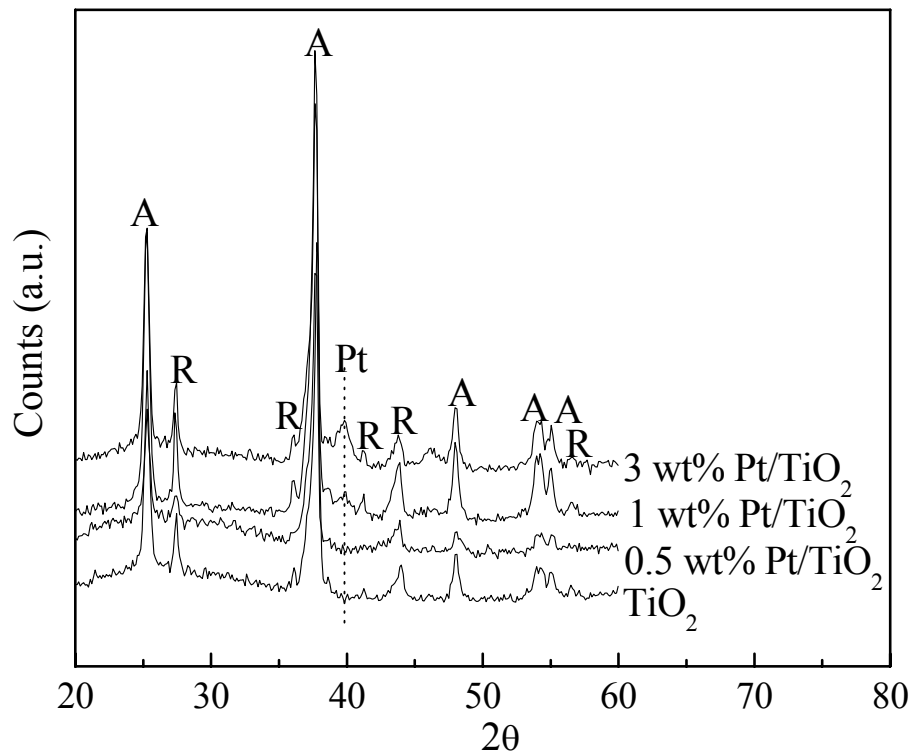


Fig. 2. XRD patterns of pure TiO<sub>2</sub>, 0.5 wt% Pt/TiO<sub>2</sub>, 1 wt% Pt/TiO<sub>2</sub> and 3 wt% Pt/TiO<sub>2</sub>. A and R designate anatase and rutile respectively.

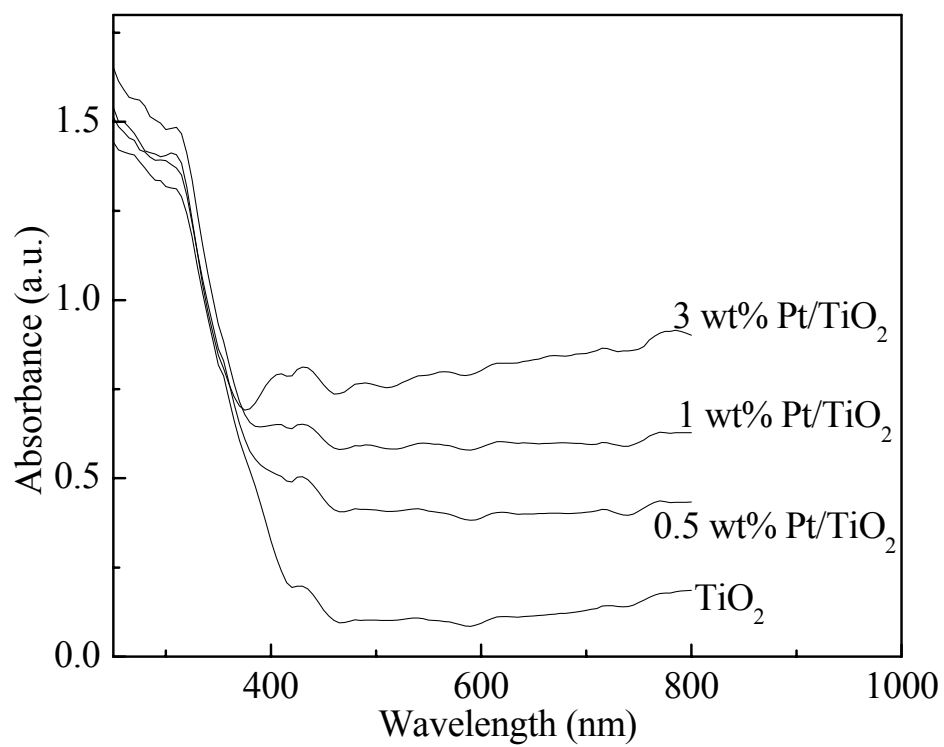


Fig. 3. UV-vis diffuse reflectance spectra of pure TiO<sub>2</sub>, 0.5 wt% Pt/TiO<sub>2</sub>, 1 wt% Pt/TiO<sub>2</sub> and 3 wt% Pt/TiO<sub>2</sub>.

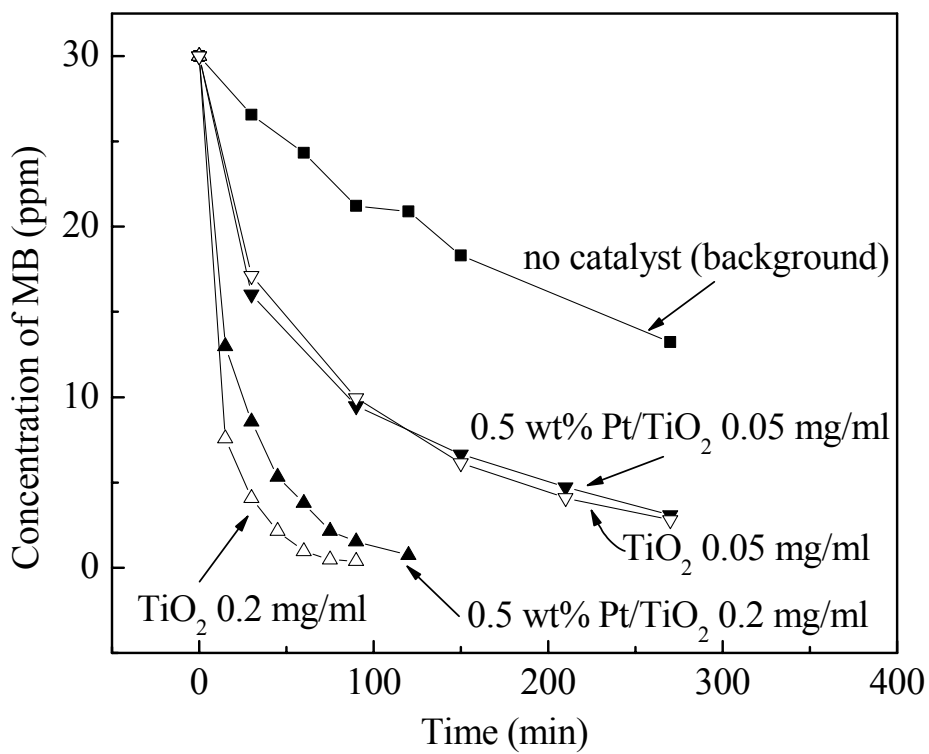


Fig. 4. Concentrations of MB as a function of time in photocatalytic oxidations of MB in aqueous solution with non-catalyst, pure TiO<sub>2</sub>,

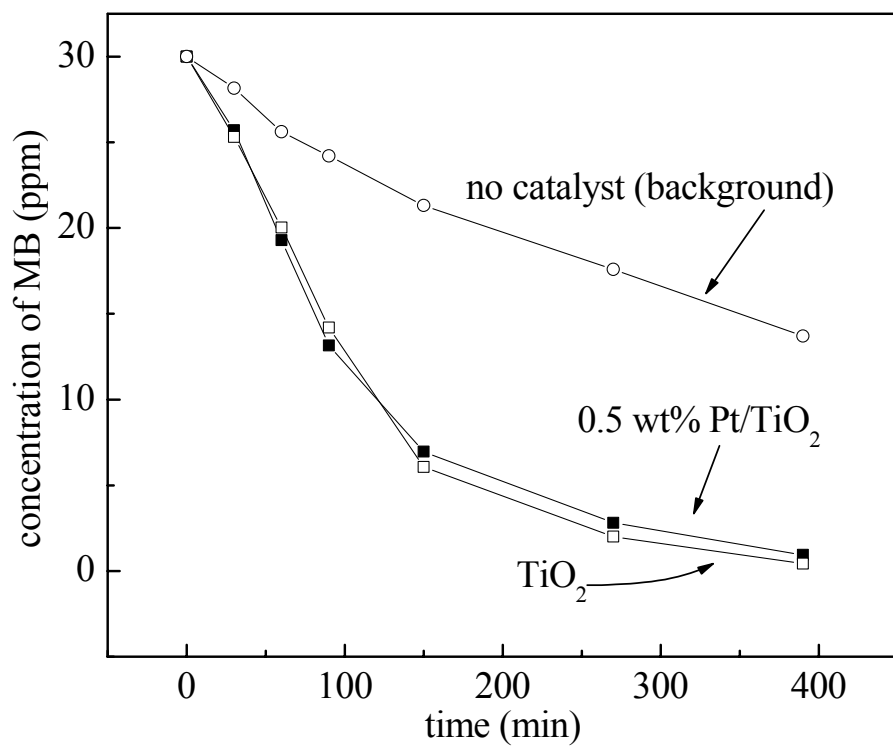


Fig. 5. Photocatalytic oxidation of MB in liquid-thin film system with non-catalyst, P25, and 0.5 wt% Pt/P25.

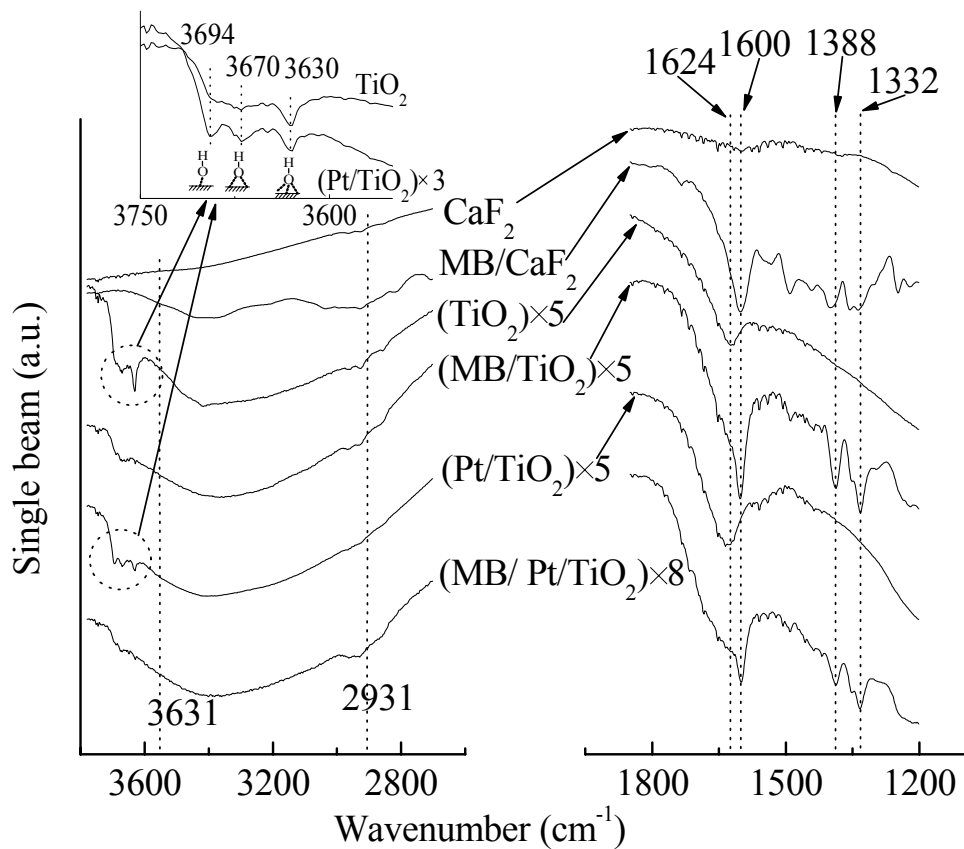


Fig. 6. IR backgrounds of CaF<sub>2</sub> and MB/CaF<sub>2</sub>, TiO<sub>2</sub> and MB/TiO<sub>2</sub>, 0.5 wt% Pt/TiO<sub>2</sub> and MB/ 0.5 wt% Pt/TiO<sub>2</sub>. The insert shows the different types of isolated hydroxyl group over TiO<sub>2</sub> and 0.5 wt% Pt/TiO<sub>2</sub> surfaces.

× indicates the spectrum is enlarged by a certain factor.

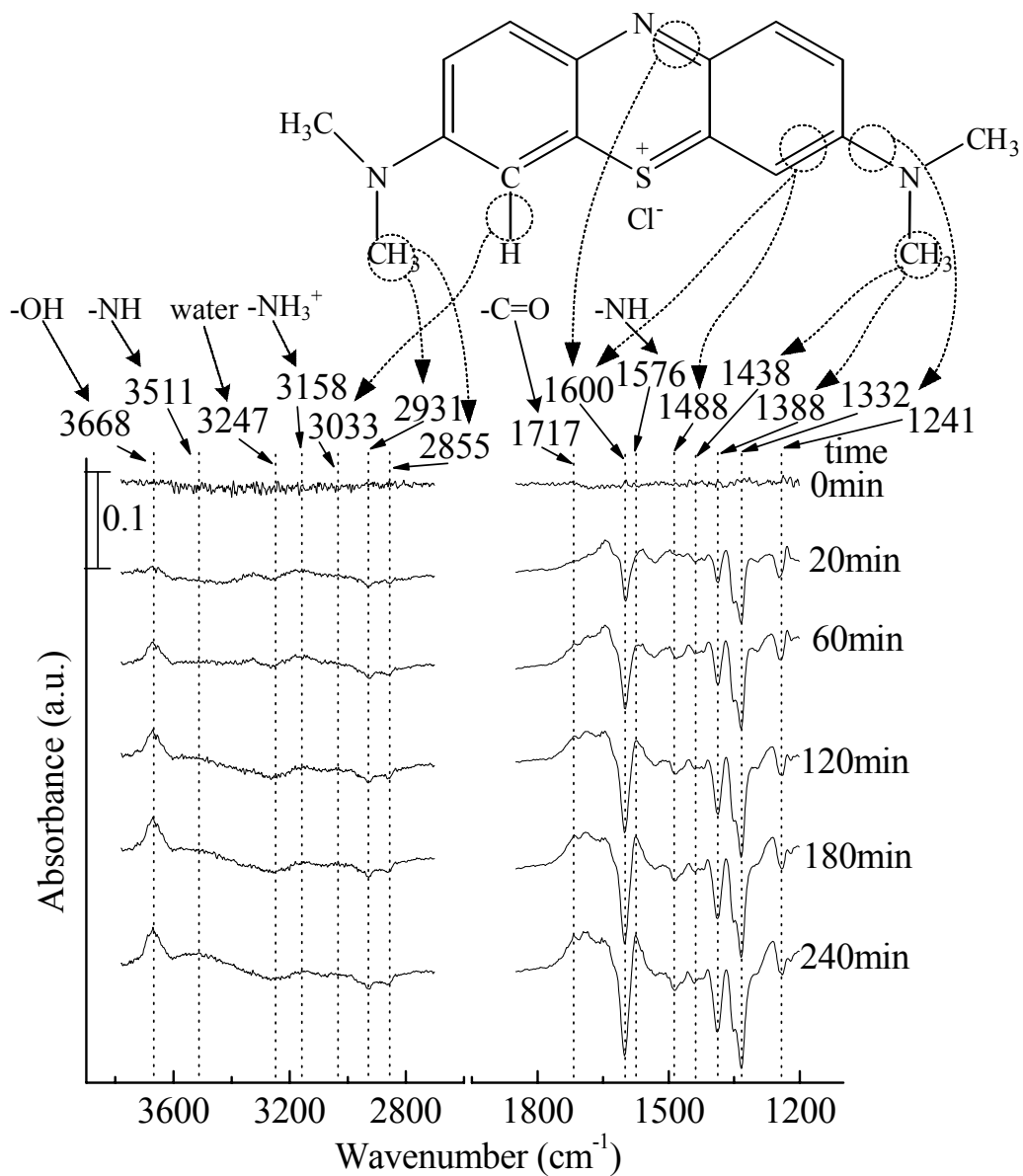


Fig. 7. In situ DRIFTS spectra and band assignments of MB photocatalytic oxidation over pure TiO<sub>2</sub> with 5 wt% MB at 1 atm

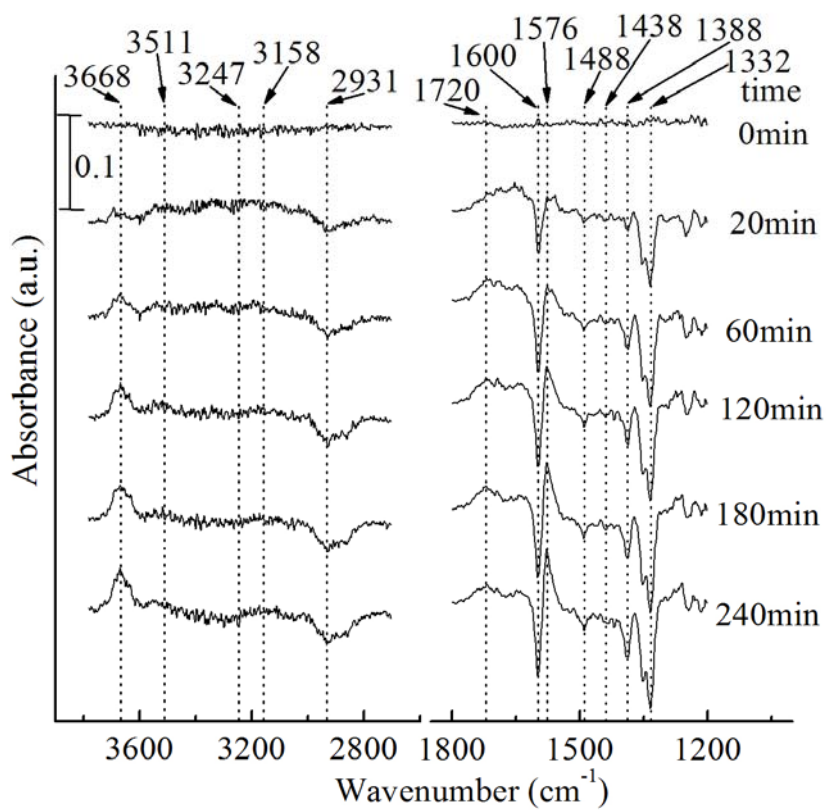


Fig. 8. In situ DRIFTS spectra of MB photocatalytic oxidation over 0.5 wt% Pt/TiO<sub>2</sub> with 5 wt% MB at 1 atm and 25 °C.

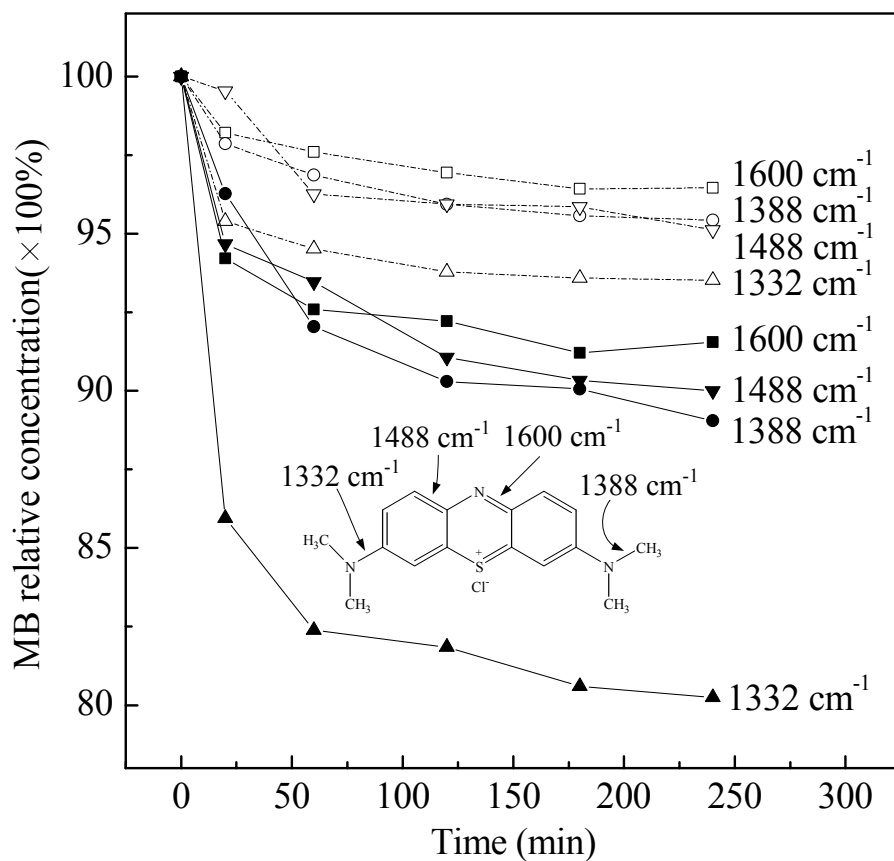


Fig. 9. Decrease rates of MB characteristic bands as a function of time in the MB photocatalytic oxidation over pure  $\text{TiO}_2$  (dash line and empty symbol) and 0.5 wt%  $\text{Pt/TiO}_2$  (black line and solid symbol) with 5 wt% MB at 1 atm and 25 °C.

**Table 1:** literature review for MB photocatalytic oxidation in aqueous solution

catalyst	Reaction conditions: $C_{MB0}$ , $C_{cat}$ , I	Kinetics model and reference reaction constant, k	reference
P25 (30nm)	$C_{MB0}=93.8 \mu\text{mol/l}$ $C_{cat}=0.2 \text{ g/l}$ $I=16.7\text{mW/cm}^2$	first-order kinetics $k=0.048 \text{ min}^{-1}$	This paper
P25 (30nm)	$C_{MB0}=100 \mu\text{mol/l}$ $C_{cat}=2 \text{ g/l}$ $I=4.7\text{mW/cm}^2$	first-order kinetics $k=0.032 \text{ min}^{-1}$	1
P25 (30nm)	$C_0=84.2 \mu\text{mol/l}$ $C_{cat}=0.5 \text{ g/l}$ $I= \text{N/A}$	first-order kinetics $k=0.053 \text{ min}^{-1}$	2
P25 (30nm)	$C_0=25 \mu\text{mol/l}$ $C_{cat}=2 \text{ g/l}$ $I: \text{N/A}$	first-order kinetics $k=0.078 \text{ min}^{-1}$	3
P25 (30nm)	$C_0=6.6 \mu\text{mol/l}$ $C_{cat}=0.67 \text{ g/l}$ $I: \text{N/A}$	first-order kinetics $k=0.0288 \text{ min}^{-1}$	4
TiO <sub>2</sub> (50 nm)	$C_0=20 \mu\text{mol/l}$ $C_{cat}=0.218 \text{ g/l}$ $I=\text{N/A}$	first-order kinetics $k=0.004 \text{ min}^{-1}$	5
TiO <sub>2</sub> (20 nm)	$C_0=31.3 \mu\text{mol/l}$ $C_{cat}=1 \text{ g/l}$ $I=\text{N/A}$	first-order kinetics $k=0.025 \text{ min}^{-1}$	6
TiO <sub>2</sub> (29.5 nm)	$C_0=39.1 \mu\text{mol/l}$ $C_{cat}=1.2 \text{ g/l}$ $I=\text{N/A}$	first-order kinetics $k=0.0188 \text{ min}^{-1}$	7
TiO <sub>2</sub> (20 nm)	$C_0=46.9 \mu\text{mol/l}$ $C_{cat}=1.2 \text{ g/l}$ $I=\text{N/A}$	first-order kinetics $k=0.0672 \text{ min}^{-1}$	8
0.75 wt% Pt/TiO <sub>2</sub> (40-80 nm)	$C_0=46.9 \mu\text{mol/l}$ $C_{cat}=1.2 \text{ g/l}$ $I=\text{N/A}$	first-order kinetics $k=0.1042 \text{ min}^{-1}$	8
TiO <sub>2</sub> (18.3 nm)	$C_0=62.6 \mu\text{mol/l}$ $C_{cat}=1.2 \text{ g/l}$ $I=\text{N/A}$	first-order kinetics $k=0.0955 \text{ min}^{-1}$	9
0.5 wt% Au/TiO <sub>2</sub> (11.8-14.2nm)	$C_0=62.6 \mu\text{mol/l}$ $C_{cat}=1.2 \text{ g/l}$ $I=\text{N/A}$	first-order kinetics $k=0.1752 \text{ min}^{-1}$	9
TiO <sub>2</sub> (18.3 nm)	$C_0=37.5 \mu\text{mol/l}$ $C_{cat}=1.2 \text{ g/l}$ $I=\text{N/A}$	first-order kinetics $k=0.0144 \text{ min}^{-1}$	10
0.5 wt% Au/TiO <sub>2</sub> (19.4 nm)	$C_0=37.5 \mu\text{mol/l}$ $C_{cat}=1.2 \text{ g/l}$ $I=\text{N/A}$	first-order kinetics $k=0.052 \text{ min}^{-1}$	10

$C_{MB0}$ : initial concentration of MB in solution.

$C_{cat}$ : concentration of catalyst in reaction solution.

I: light intensity.

**Table 2:** assignment of the FTIR bands observed in MB photocatalytic oxidation over  $TiO_2$  at 1 atm and 25 °C.

Frequency ( $cm^{-1}$ )	Vibration mode of functional group
3668	-OH
3511	-NH
3247	Absorbed water
3158	$-NH_3^+$
3033	Aromatic C-H
2931	-CH <sub>3</sub> asymmetric stretching
2855	-CH <sub>3</sub> symmetric stretching
1718	-C=O
1600	C=N/C=C
1576	-N-H
1488	C=C
1438	-CH <sub>3</sub> asymmetric deformation
1388	-CH <sub>3</sub> symmetric deformation
1333	Aromatic amines, $C_{Ar}$ -N